

## MICROSTRUCTURAL AND MECHANICAL CHARACTERIZATION OF LASER POWDER BED FUSION OF IN718 OVERHANGS

M. Hanumantha\*, B. Farhang\*, B. B. Ravichander\*, A. Ganesh-Ram\*, S. Ramachandra\*, B. E.  
Finley\*, N. Swails<sup>†</sup>, A. Amerinatanzi\*<sup>†</sup>

\*Mechanical & Aerospace Engineering, University of Texas at Arlington, Arlington, TX.

<sup>†</sup>Math, Science, Nursing, and Public Health, University of South Carolina Lancaster, SC.

<sup>†</sup>Materials Science and Engineering, University of Texas at Arlington, Arlington, TX.

### Abstract

Inconel 178 (IN718), a nickel-chromium-based superalloy known for its superior properties is used in aerospace, oil, and gas industries. Due to its high hardness, IN718 is difficult to be machined. Therefore, fabrication of IN718 components with complex geometries is a big challenge when conventional manufacturing techniques are used. Laser powder bed fusion (LPBF) technique can be used to fabricate IN718 parts with high precision. During fabrication of overhang structures, supports are typically employed, which significantly increases the use of resources such as material consumption and postprocessing. The focus of this study is to determine the angle at which an overhang structure can be fabricated without employing supports. To this aim, the angled-overhang samples with varied angles (30°-90°) were manufactured with no support. The effect of overhang state on the microstructural and mechanical properties of the LPBF-processed IN718 samples was analyzed. According to the microstructural analysis, the deepest melt pools in the overhang sample seemed to be at a hanging angle of 45°. Moreover, the overhang sample fabricated at 45° had the greatest Vickers hardness value of 382.90 HV. This study urges a reconsideration of the common approach of selecting supports for overhang samples in the LPBF process when a higher quality of the as-fabricated parts is desired.

**Keywords:** Laser powder bed Fusion, Overhangs, IN718, Microstructure, Vickers Hardness.

### 1. Introduction

The requirement for a strengthened, non-hardenable alloy with a high melting point of 1200°F to 1400°F (650°C to 760°C) opened the way for the development of Inconel718 (IN718) [1, 2]. In the early phases of manufacturing for Ni-based superalloys, stability was considered to be a crucial condition. IN718 is an age-hardenable Ni-Cr austenitic alloy having a work temperature range of 257 °C to 704 °C [3-8]. The crystallization of Ni and Cr in phase aids corrosion resistance. The precipitation of Ni<sub>3</sub>Nb into the  $\gamma''$  process results in the hardening of the alloy [9, 10]. This hardening makes the machinery of IN718 products a challenging task more specifically for producing complex geometry.

The laser powder bed fusion technique (LPBF) is one of the most commonly used metal additive manufacturing (AM) techniques for fabrication of Inconel 718 (IN718) with complex geometry [5, 11-14]. Layer-by-layer of pre-spread powders are used in LPBF processes to create a dense three-dimensional component directly from user-defined CAD data. Despite the well-known

advantages and the availability of commercial LPBF systems on the global market, LPBF still faces many obstacles, and the speed of part fabrication and the maximum part size that may be made limit the technology's affordability and widespread adoption [15, 16].

While LPBF provides a high degree of geometrical flexibility, overhang structure in a target part requires special attention for effective fabrication. Overhang supports are used in LPBF process to build parts and conduct energy from the melt pool to the build plate, which aids in providing stable thermal conditions for the LPBF operation. Jingchao Jiang *et al.* [17] worked on understanding the importance of support structures in AM and proposed it as a critical parameter for an effective fabrication of part. As they reported, supporting structures minimizes deformation in parts while still performing other tasks such as heat removal and sample fabrication. Though supports are necessary, implementing them would require a significant number of resources, and creating suitable supports could be tedious and time-consuming. Supports influence roughness, mechanical properties, material use, and microstructural properties, with improvement in the hardness value being observed for the parts fabricated with supports compared to the samples manufactured without supports [18]. Additionally, to remove the supports, postprocessing procedures are necessary, and surface smoothing processes are recommended for the part [19]. Tolosa *et al.* [20] investigated the variation of tensile properties for inclined samples fabricated with a base geometry in the Z-X to Z-Y plane and the main axis of the sample angled with respect to the z direction. Tensile tests conducted on inclined samples fabricated at various angles with supports revealed that the 45° overhang angle had the highest strength properties.

The motivation of this study is to determine the angle at which an overhang structure can be fabricated without employing supports, without sacrificing the quality and performance of LPBF-fabricated parts. To this aim, angled-overhang samples with varied angles (30°-90°) were fabricated using an EOS M290 metal printer. The effects of different overhang angles on the microstructure and mechanical properties were investigated systematically through SEM and Vickers hardness test, respectively.

## **2. Materials and Methods**

The samples under study were modeled in Solidworks 2019 software (version 2018-2019, Dassault Systems, USA). Samples were built in the form of a corner angled bracket, with varying angles (45°, 60°, 75° and 90°) on one side of the angled corner with a constant thickness of 4 mm. The samples were labeled based on the geometrical factors (angle-A and thickness T) in this study as A45T4, A60T4, A75T4 and A90T4. The design's base area was set to 10×5 mm, with a base thickness of 2 mm for all samples.

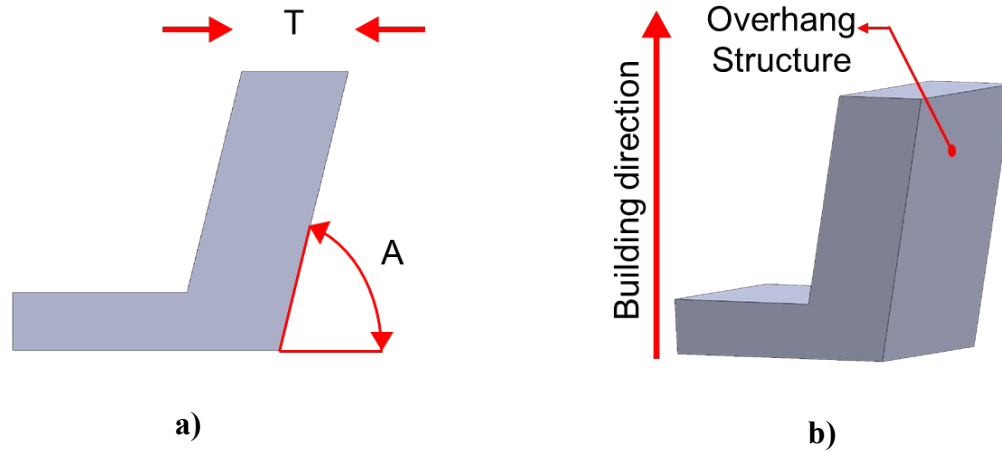


**Figure 1.** a) geometrical variations (angle) considered in designing the CAD file; b) 3D view of the CAD model.

The IN718 powder comprised of Ni (55 wt.-%), Cr (17 wt.-%), Nb (4.75 wt.-%), Mo (3.3 wt.-%) was obtained from EOS (EOS GmbH, Electro Optical Systems, Krailling, Germany). The particle size in the powder was around 35-40  $\mu\text{m}$  and had a relative density of  $\sim 100\%$ . For the fabrication of the samples, an EOS M290 DMLS metal 3D printer (EOS GmbH, Electro Optical Systems, Krailling, Germany) was equipped with a 400 W Ytterbium fiber laser was used. The laser processing parameters chosen for this study were 285-Watt laser power (P), 960 mm/s scanning speed ( $v$ ), 110  $\mu\text{m}$  hatch spacing (h), and 40  $\mu\text{m}$  layer thickness, with an energy density of 67  $\text{J}/\text{mm}^3$ .

The samples were removed from the building plate after fabrication. The main sample was cut using an Allied Techcut 4<sup>TM</sup> precision cutter, and the base area was separated by a plane parallel to the building direction. A consistent polishing process was employed to maintain consistency in the as-fabricated components being prepared for SEM analysis. The E-prep 4<sup>TM</sup> polisher was used in combination with polishing sandpaper of grits 180, 320, 600, 800, and 1200 to obtain the first polished surface with water as a lubricant. Following this standard procedure, a 'DiaMat' polishing cloth with a 1  $\mu\text{m}$  polycrystalline diamond suspended solution was employed, and a 0.5  $\mu\text{m}$  colloidal silica solution was applied with a 'Red Final C' polishing cloth. Each polishing cycle was performed twice, for a total of 10 minutes.

A Hitachi S-3000N scanning electron microscope (SEM) was used to test the sides of the overhang samples on the microstructure of the fabricated main parts. SEM imaging was conducted on all 4 main samples near the support zone (on the polished side surface). To test the effect of the overhang angle on the mechanical properties of the samples, the Vickers hardness test was conducted with the help of a Leco LM 300 AT microhardness tester under an applied load of 500 g for 10 seconds. A total of 4 indentations were performed on each specimen to declare the average hardness value.

### **3. Results and Discussion**

#### **3.1 Microstructure Analysis**

In Figure 2, the SEM image of the side surface of the main parts along the building path is presented. Due to the laser beam passes of each layer, the images show melt pools with a Gaussian form. As shown in Table 1, different overhang angles ( $A$ ) have an impact on the melt pool width and depth in the side surface of each fabricated sample. For the as-fabricated samples with constant thickness and varying angles of  $45^\circ$ ,  $60^\circ$ ,  $75^\circ$ , and  $90^\circ$ , no significant relationship between variation in melt pool size was observed. However, a change in the dimension of the pools was observed between samples. The results of the dimensional analysis performed on the last fabricated layer of the melt pools are presented in Figure 3. In terms of the depth of the pools, no specific trend was found as the angle of the overhang structure increased. With increasing the angle from  $45^\circ$  (A45T4) to  $60^\circ$  (A60T4), a significant decrease in the depth of the pools was revealed. By contrast, deeper pools were formed for the sample with  $75^\circ$  overhang angle (A75T4). It is noted that more increase in overhang angle did not change the depth of the pools, as a similar average value was found for the sample with straight overhang (A90T4). Moreover, the analysis of the width of the pools showed no particular trend for the samples fabricated with different overhang angle. In this case, the widest pools were formed in the sample with  $45^\circ$  overhang angle (A45T4), with a considerable decrease in width of the pools being found when the angle increased to  $60^\circ$  (A60T4). However, width of the pools increased as the angle increased from  $60^\circ$  (A60T4) to  $75^\circ$  (A75T4). This upward trend did not continue as narrower pools were observed for the sample fabricated with straight overhang structure (A90T4) compared to the sample with  $75^\circ$  overhang angle (A75T4). From  $45^\circ$  to  $90^\circ$  no significant relationship was found between variation in melt pool size and overhang angle. However, a decrease in melt pool width and depth was observed. The average melt pool width varied from  $128.56 \mu\text{m}$  to  $116.22 \mu\text{m}$  and the average melt pool depth varied from  $54.66 \mu\text{m}$  to  $65.96 \mu\text{m}$ . As per the results bigger melt pools were observed at  $45^\circ$  inclination and smaller melt pools were observed at  $90^\circ$  inclination. This is because the surface area of the fabricated layer at lower inclination is greater compared to the samples fabricated at higher inclination.

The variation in the dimension of the pools, which can be inferred as the variation in microstructure of the samples, can be attributed to the different inclination angles used in the overhang structures. Chen *et al.* [21] showed that change in the inclined angle in overhang structures can lead to a different overhanging length, thereby resulting in a different level of staircase effect during the fabrication. It was also mentioned that the staircase effect has an adverse impact on the quality of the overhanging structures. In another study performed by Wang *et al.* [22], the influence of inclined angle on the properties of LPBF fabricated parts was investigated. By changing the angle between  $25^\circ$  to  $45^\circ$ , the authors proved that a different inclined angle in overhang structures brings about different quality for the parts. It was concluded the process parameters (particularly scanning speed) should be adjusted based on the inclined angle to obtain the ideal quality for the overhang structures. A similar observation was reported in another study [23], as it was concluded that LPBF technique is capable of fabrication of overhanging structures by selecting proper scan strategies and process parameters. This confirmed the variation in microstructure observed for the samples in this study, as different inclination angles but same process parameters were used for the overhang structures. More investigation is needed to find the specific relationship between the overhanging angle and microstructure features of the parts.

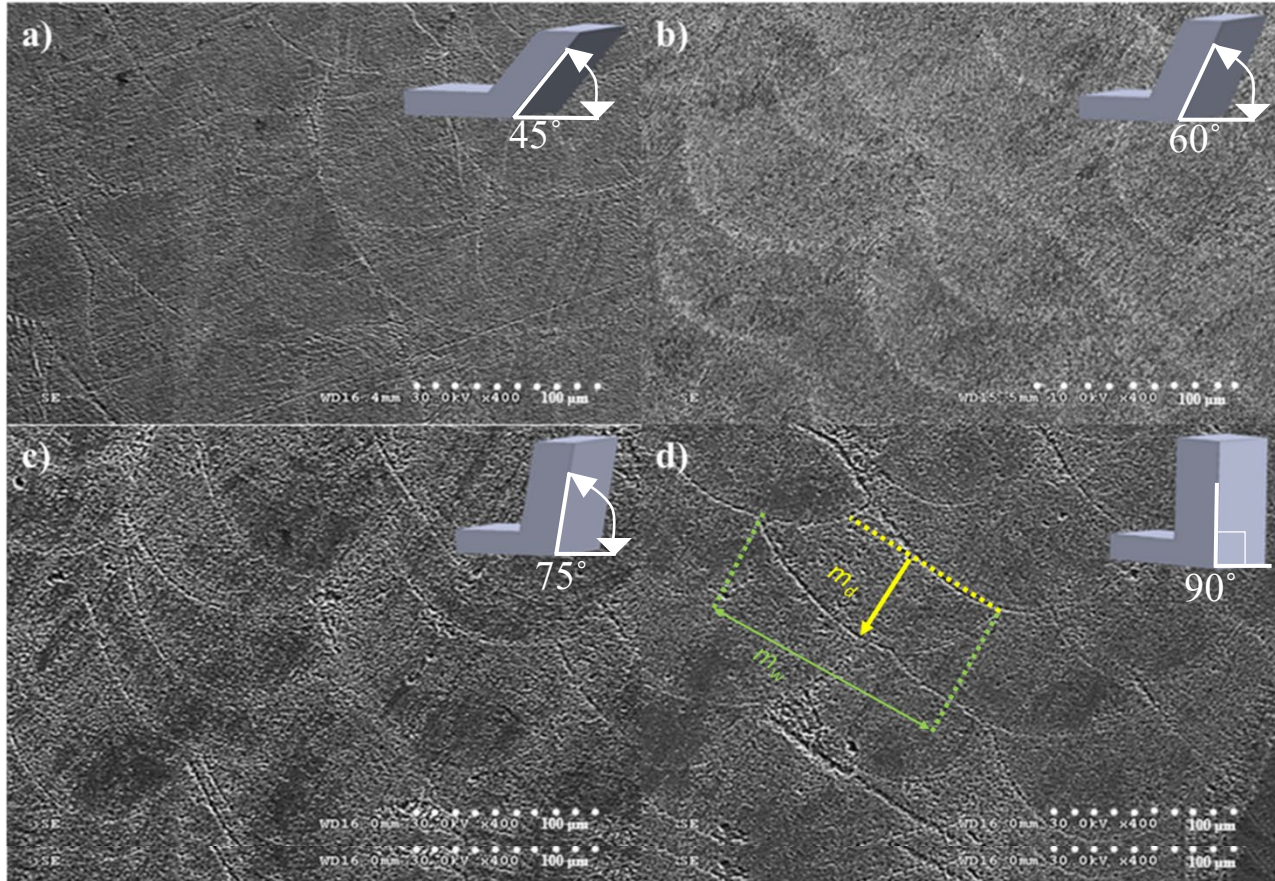


**Figure 2.** SEM images of meltpool depth ( $m_d$ ) and meltpool width ( $m_w$ ) for a) A45T4; b) A60T4; c) A75T4; d) A90T4.

### 3.2 Hardness Analysis

Vickers hardness tests were conducted on each sample at the bottom of the overhang to determine the impact of the angle on the as-built specimens. As can be seen in Figure 3, with increased incline angle, the hardness of the fabricated overhangs samples decreases. According to the results, Vickers hardness was determined to be 382.90 HV, 373.02 HV, 347.15 HV and 341.55 HV for samples A45T4, A60T4, A75T4 and A90T4, respectively. It has been revealed that with more overlap between the melt pools and formation of deeper pools, more reheating cycles occur which has similar effect as the heat treatment process. This, thereby, results in higher hardness values [24-26]. However, according to the results presented in the previous section, no specific trend was observed for the depth of the melt pools. Therefore, the trend was observed for the hardness of the samples can be attributed to the energy density level, which has been shown to have a strong relationship with the hardness value. It has also been reported there is an inverse relationship between micro hardness and level of defects [27]. With increasing the angle from 45 (A45T4) to 90 (A90T4), the surface area in contact with laser energy reduces which then increases the heat dissipation and cooling rate. Yilmaz *et al.* [28] investigated the effect of cooling rate on the quality of LPBF processed parts and concluded that by increasing the cooling rate, the possibility of formation of defects in the part increases. They suggested diminishing the cooling rate throughout the part with increasing the surface area. Therefore, with decrease in the inclination

angle and with a larger surface area, a lower level of defects and higher hardness value are expected for the samples, which is consistent with the presented results. However, increase in cooling rate also results in grain refinement contradicts to our observation. More investigation is needed to find the effect of overhang angle on the grain size and then the hardness value.

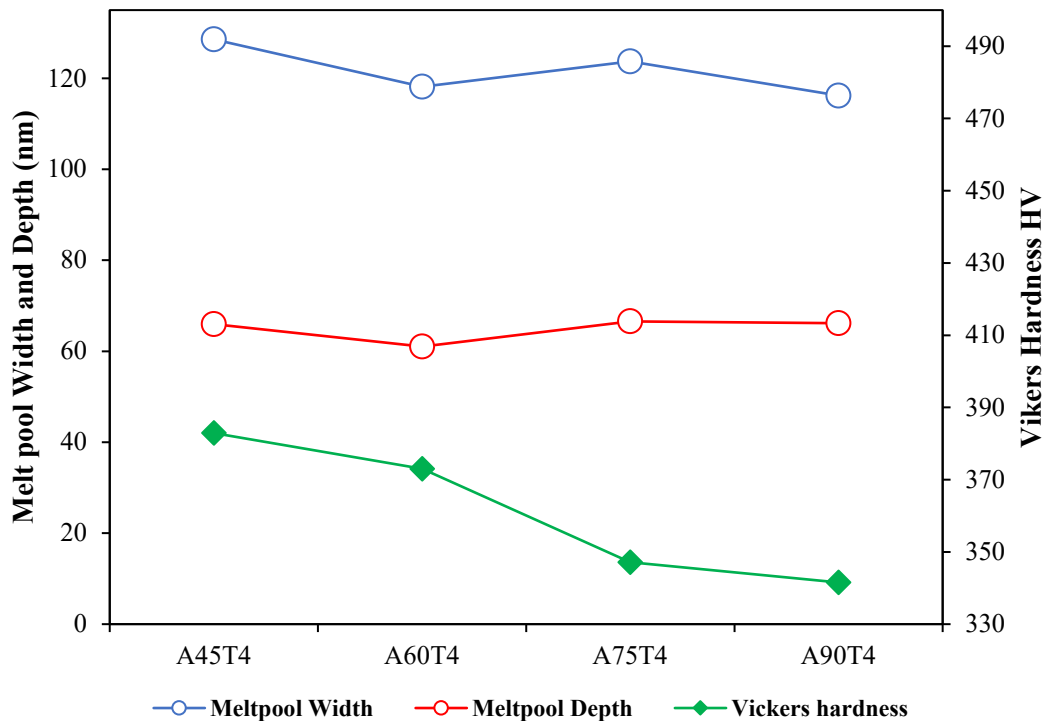


**Figure 3.** Melt pool width, Depth, Vickers hardness results for all 4 overhang IN718 samples with varying angles.

#### **4. Conclusion**

LPBF of IN718 overhang structures and the effect of inclined angle on the microstructure and hardness properties were studied. The following observations were made based on the results of this study.

1. No significant change in the structure (melt pool boundaries) of the melt pools was found for the samples fabricated with constant thickness and varying angle.
2. Dimensional analysis of the melt pools revealed microstructure variation in terms of width and depth between the samples fabricated with different inclined angles.
3. In terms of dimensions of the pools, the deepest and widest pools were found for the samples with 75 (A75T4) and 45 (A45T4) inclined angles, respectively. Moreover, no specific relationship was found between the melt pool dimensions and the overhang angle. A detailed study with limited range of overhang angle should be conducted to investigate this relationship.

4. Finally, the micro hardness results showed a strong relationship with the inclined angle. As the angle of the overhangs increased, the hardness values dropped.

## 5. References

1. Hanumantha, M.a.R., Bharath Bhushan and Singh, Manya and Swails, Nahid and Amerinatanzi, Amirhesam, *Spatial microstructural analysis for selective laser melted components*, in *International Society for Optics and Photonics*. 2021, International Society for Optics and Photonics. p. 115890L.
2. Ganesh-Ram, A.a.R., Samarth and Ravichander, Bharath Bhushan and Swails, Nahid and Amerinatanzi, Amirhesam, *Study on the microstructural and hardness variations of unsupported overhangs fabricated using selective laser melting*. 2021. **11589**: p. 1158900.
3. Lingenfelter, A., *Welding of Inconel alloy 718: A historical overview*. Superalloy, 1989. **718**: p. 673-683.
4. Metals, S., *Inconel alloy 718*. Publication Number SMC-045. Special Metals Corporation, 2007.
5. Bharath Bhushan, R., A. Amirhesam, and M. Narges Shayesteh. *Toward mitigating microcracks using nanopowders in laser powder bed fusion*. in *Proc.SPIE*. 2021.
6. Bharath Bhushan, R., et al. *Development of ANN model for surface roughness prediction of parts produced by varying fabrication parameters*. in *Proc.SPIE*. 2021.
7. Farhang, B., et al., *Study on variations of microstructure and metallurgical properties in various heat-affected zones of SLM fabricated Nickel–Titanium alloy*. *Materials Science and Engineering: A*, 2020. **774**: p. 138919.
8. Vignesh, R.K.R., et al. *Determination of residual stress for Inconel 718 samples fabricated through different scanning strategies in selective laser melting*. in *Proc.SPIE*. 2020.
9. Lewandowski, M.a.S., V and Wilcox, RC and Matlock, CA and Overfelt, RA, *High temperature deformation of Inconel 718 castings*. *Superalloys*, 1994. **718**: p. 625--706.
10. Wang, Z.a.R., Kamalakar P and Fan, J and Lei, S and Shin, YC and Petrescu, G, *Hybrid machining of Inconel 718*. *International Journal of Machine Tools and Manufacture*, 2003. **43**: p. 1391--1396.
11. Wong, K.V. and A. Hernandez, *A review of additive manufacturing*. *International scholarly research notices*, 2012. **2012**.
12. Ravichander, B.B., A. Amerinatanzi, and N. Shayesteh Moghaddam, *Study on the Effect of Powder-Bed Fusion Process Parameters on the Quality of as-Built IN718 Parts Using Response Surface Methodology*. *Metals*, 2020. **10**(9).
13. Bharath Bhushan, R., et al. *Analysis of the deviation in properties of selective laser melted samples fabricated by varying process parameters*. in *Proc.SPIE*. 2020.
14. Ravichander, B.B., et al., *A Prediction Model for Additive Manufacturing of Inconel 718 Superalloy*. *Applied Sciences*, 2021. **11**(17).
15. Bourell, D.L.a.R., David W and Leu, Ming C, *The roadmap for additive manufacturing and its impact*. *3D Printing and Additive Manufacturing*, 2014. **1**: p. 6--9.

16. Gao, W.a.Z., Yunbo and Ramanujan, Devarajan and Ramani, Karthik and Chen, Yong and Williams, Christopher B and Wang, Charlie CL and Shin, Yung C and Zhang, Song and Zavattieri, Pablo D, *The status, challenges, and future of additive manufacturing in engineering*. Computer-Aided Design, 2015. **69**: p. 65--89.
17. Jiang, J., X. Xu, and J. Stringer, *Support structures for additive manufacturing: a review*. Journal of Manufacturing and Materials Processing, 2018. **2**(4): p. 64.
18. Ameen, W.a.A.-A., Abdulrahman and Mohammed, Muneer Khan, *Self-supporting overhang structures produced by additive manufacturing through electron beam melting*. The International Journal of Advanced Manufacturing Technology, 2019. **104**: p. 2215--2232.
19. Thakare, S.H., *Experimental investigation of effect of support structure geometry on the microstructure and metallurgical properties of IN718 parts fabricated by selective laser melting*, in *Mechanical and Aerospace Engineering*. 2020, The University of Texas at Arlington.
20. Tolosa, I.a.G.i.a., Fern{\i}n and Zubiri, Fidel and Zapirain, Fidel and Esnaola, Aritz, *Study of mechanical properties of AISI 316 stainless steel processed by "selective laser melting", following different manufacturing strategies*. The International Journal of Advanced Manufacturing Technology, 2010. **51**: p. 639--647.
21. Chen, H., et al., *Improving additive manufacturing processability of hard-to-process overhanging structure by selective laser melting*. Journal of Materials Processing Technology, 2017. **250**: p. 99-108.
22. Wang, D., et al., *Research on the fabricating quality optimization of the overhanging surface in SLM process*. The International Journal of Advanced Manufacturing Technology, 2013. **65**(9-12): p. 1471-1484.
23. Cloots, M., et al., *Approaches to minimize overhang angles of SLM parts*. Rapid Prototyping Journal, 2017.
24. Amato, K.a.G., SM and Murr, Lawrence E and Martinez, Edwin and Shindo, PW and Hernandez, J and Collins, S and Medina, F, *Microstructures and mechanical behavior of Inconel 718 fabricated by selective laser melting*. Acta Materialia, 2012. **60**: p. 2229--2239.
25. Wang, Z.a.G., Kai and Gao, Ming and Li, Xiangyou and Chen, Xiaofeng and Zeng, Xiaoyan, *The microstructure and mechanical properties of deposited-IN718 by selective laser melting*. Journal of alloys and compounds 2012. **513**: p. 518--523.
26. Zhang, D.a.N., Wen and Cao, Xuanyang and Liu, Zhen, *Effect of standard heat treatment on the microstructure and mechanical properties of selective laser melting manufactured Inconel 718 superalloy*. Materials Science and Engineering: A, 2015. **644**: p. 32--40.
27. Tucho, W.M., et al., *Investigation of effects of process parameters on microstructure and hardness of SLM manufactured SS316L*. Journal of Alloys and Compounds, 2018. **740**: p. 910-925.
28. Yilmaz, N. and M.Y. Kayacan, *On The Relation Between Cooling Rate and Parts Geometry in Powder Bed Fusion Additive Manufacturing*. Academic Perspective Procedia, 2018. **1**(1): p. 223-231.